Biogeosciences Discuss., 11, 4995–5021, 2014
www.biogeosciences-discuss.net/11/4995/2014/
doi:10.5194/bgd-11-4995-2014

Biogeosciences
Discussions
Open Access

Disentangling residence time and temperature sensitivity of microbial decomposition in a global soil carbon model

J.-F. Exbrayat[1,*], A. J. Pitman[1], and G. Abramowitz[1]

[1] ARC Centre of Excellence for Climate System Science and Climate Change Research Centre, University of New South Wales, Sydney, New South Wales, Australia
[*] now at: School of GeoSciences and National Centre for Earth Observation, University of Edinburgh, Edinburgh, UK

Received: 5 February 2014 – Accepted: 24 March 2014 – Published: 31 March 2014

Correspondence to: J.-F. Exbrayat (j.exbrayat@ed.ac.uk)

Published by Copernicus Publications on behalf of the European Geosciences Union.

Abstract

Recent studies have identified the first-order parameterization of microbial decomposition as a major source of uncertainty in simulations and projections of the terrestrial carbon balance. Here, we use a reduced complexity model representative of the current state-of-the-art parameterization of soil organic carbon decomposition. We undertake a systematic sensitivity analysis to disentangle the effect of the time-invariant baseline residence time (k) and the sensitvity of microbial decomposition to temperature (Q_{10}) on soil carbon dynamics at regional and global scales. Our simulations produce a range in total soil carbon at equilibrium of ~592 to 2745 Pg C which is similar to the ~561 to 2938 Pg C range in pre-industrial soil carbon in models used in the fifth phase of the Coupled Model Intercomparison Project. This range depends primarily on the value of k, although the impact of Q_{10} is not trivial at regional scales. As climate changes through the historical period, and into the future, k is primarily responsible for the magnitude of the response in soil carbon, whereas Q_{10} determines whether the soil remains a sink, or becomes a source in the future mostly by its effect on mid-latitudes carbon balance. If we restrict our simulations to those simulating total soil carbon stocks consistent with observations of current stocks, the projected range in total soil carbon change is reduced by 42 % for the historical simulations and 45 % for the future projections. However, while this observation-based selection dismisses outliers it does not increase confidence in the future sign of the soil carbon feedback. We conclude that despite this result, future estimates of soil carbon, and how soil carbon responds to climate change should be constrained by available observational data sets.

1 Introduction

There is a 6-fold range in the amount of carbon stored in the soil in simulations conducted as part of the fifth phase of the Coupled Model Intercomparison Project (CMIP5; Taylor et al., 2012). This 6-fold range, identified by Todd-Brown et al. (2013), is consistent with results from the recent model intercomparison projects such as the Coupled Climate–Carbon Cycle Model Intercomparison Project (C^{4}MIP; Friedlingstein et al., 2006). The analysis of carbon stores in both C^{4}MIP and CMIP5 have focused on the prediction of terrestrial and soil carbon through time. In addition to demonstrating the large differences in carbon stocks (Todd-Brown et al., 2013), they have also highlighted large inter-model differences in global and regional land–atmosphere carbon (C) fluxes (e.g. Friedlingstein et al., 2006, 2014). This lack of agreement between simulations exists in fully coupled models (e.g. C^{4}MIP and CMIP-5) but can also be found if sources of uncertainty are narrowed by relying on one weather dataset to drive multiple land models (Friend et al., 2014; Nishina et al., 2013), or by using one land model driven by multiple climate projections (Ahlström et al., 2013).

In these previous studies, critical uncertainties have been identified in the microbial decomposition of soil organic C and the associated release of CO_2 via heterotrophic respiration (R_h). This is despite all the current state-of-the-art global soil C models relying on a similar parameterization of decomposition as a first-order process (see Exbrayat et al., 2013b; Nishina et al., 2013; Todd-Brown et al., 2013). This conceptualization describes decomposition and R_h as proportional to the availability of organic matter. The decay rate (or R_h per unit of soil C) is modified based on an environmental scalar that intends to mimic the dynamical response of microbial biomass to soil moisture and soil temperature.

This simple parameterization has recently received some criticism because of its lack of explicit representation of microbial physiology (Allison et al., 2010; Todd-Brown et al., 2012; Wieder et al., 2013; Xenakis and Williams, 2014). However, it can successfully explain some complex dynamic processes including the acclimation of decomposers to warming (Luo et al., 2001) as a result of the quick depletion of labile pools by enhanced microbial biomass (Kirschbaum, 2004; Knorr et al., 2005).

We previously identified (Exbrayat et al., 2013b) some further implications of the first-order parameterization of microbial decomposition. First, in climate change experiments, model pools are usually initialised using a spin-up procedure with fixed pre-industrial atmospheric CO_2 concentrations until C pool trends are removed (Xia et al., 2012). Due to the interaction with substrate availability, the decay rate simulated by the model in response to steady boundary conditions determines the size of soil C pools reached at equilibrium. Because spin-up is a long computational process, the magnitude of pool sizes is conserved during subsequent shorter simulations of climate change and, as a result, equilibrated stocks strongly explain final stocks (e.g. CMIP5 models as shown in Fig. S1). Second, the microbial sensitivity to changing environmental conditions affects the response of the system under transient climate simulations (Falloon et al., 2011; Exbrayat et al., 2013a, b). However, because substrate availability also controls the amount of respired carbon, there is a "memory" control imposed by the initial conditions of this transient simulation (Exbrayat et al., 2013b) that also affects the response to perturbation in boundary conditions. The relative contribution of these two factors on soil C projections remains to be explored in detail especially since last generation models disagree on the carbon balance projected in the future (Friedlingstein et al., 2014; Nishina et al., 2013), making it challenging to elaborate any land-based offsetting strategy.

Here, we use a reduced complexity model representative of the current state-of-the-art parameterization of soil organic C decomposition. A systematic sensitivity analysis is performed to disentangle the effect of the time-invariant baseline residence time and the formulation of the dynamic response of microbial decomposition to climatic change on soil C dynamics at regional and global scale.

2 Materials and methods

2.1 Reduced complexity model

It is not possible to re-run each CMIP5 model or isolate the representation of soil carbon processes from each model. We therefore use a reduced complexity model that simulates the monthly evolution of a single soil organic carbon pool, C_s, in response to input derived from Net Primary Productivity (NPP, $\mathrm{g\,C\,m^{-2}\,mth^{-1}}$) and output by heterotrophic respiration (R_h, $\mathrm{g\,C\,m^{-2}\,mth^{-1}}$). For each monthly time step, the soil carbon balance can be described as:

$$\frac{\partial C_\mathrm{s}}{\partial t} = \mathrm{NPP} - R_\mathrm{h} \tag{1}$$

where NPP is a prescribed boundary condition in our model and R_h is simulated as a first-order process dependent on the availability of substrate C_s such as:

$$R_\mathrm{h} = k^{-1} \times f_\mathrm{T} \times f_\mathrm{W} \times C_\mathrm{s} \tag{2}$$

where k is the baseline residence time at 15 °C (Xia et al., 2013) adjusted at each time step by f_T which is a function of soil temperature T_s (°C). The soil moisture (θ_s) modification function, f_W, is usually expressed as a fraction of soil moisture saturation (Moyano et al., 2012). We implement a classical formulation of the soil temperature sensitivity function f_T:

$$f_\mathrm{T} = Q_{10}^{\frac{(T_\mathrm{s}-T_\mathrm{ref})}{10}} \tag{3}$$

where Q_{10} is a constant factor that describes the relative increase in microbial activity for a warming of 10 °C, and T_ref is the reference temperature (°C) for which $f_\mathrm{T}(T_\mathrm{s}) = 1$ (Lloyd and Taylor, 1994; Bauer et al., 2012). The chosen T_ref is the commonly used 15 °C (Todd-Brown et al., 2013) so that the decomposition rate equals k^{-1} when moisture is non-limiting and temperature is approximately equal to the global average. We use the same formulation of f_W as in the CASA-CNP model (Wang et al., 2010):

$$f_\mathrm{W}(\theta_\mathrm{s}) = \left(\frac{\theta_\mathrm{s} - 1.70}{0.55 - 1.70}\right)^{6.6481} \times \left(\frac{\theta_\mathrm{s} + 0.007}{0.55 + 0.007}\right)^{3.22} \tag{4}$$

which is a bell-shaped function that is equal to 1 for $\theta_\mathrm{s} = 0.55$.

This first-order representation of microbial decomposition with a specified decay rate adjusted by environmental scalars is used in all 17 CMIP5 models that simulate soil carbon (Todd-Brown et al., 2013) and all 7 Dynamic Global Vegetation Models used in the ISI-MIP project (Friend et al., 2014; Nishina et al., 2013). Typically, these models rely on a multi-pool architecture to represent the diversity in organic matter. Each pool has its own residence time that corresponds to a degree of resistance to decomposition (Davidson and Janssen, 2006). Usually, part of the decomposition occurring in one pool is routed to one or several other pools while the rest is emitted via R_h. At the ecosystem scale, however, the same environmental scalar is applied despite the multi-pool architecture, and the heterotrophic respiration flux is proportional to the amount of substrate available. Therefore, our simplified model is broadly representative of the current paradigm and provides a useful framework to undertake the sensitivity analysis described hereafter.

We are also aware that soil moisture has an influence on microbial decomposition (Falloon et al., 2011; Moyano et al., 2012, 2013; Exbrayat et al., 2013a, b). However, Todd-Brown et al. (2013) recently demonstrated that a one pool reduced complexity model could reproduce both total soil carbon content and its spatial distribution for most of the CMIP5 models without considering decomposition response to variations in soil moisture. We also recently showed that global features in the distribution and evolution of C_s were much more related to uncertainties in f_T than uncertainties in the formulation of f_W (Exbrayat et al., 2013b). Therefore, in order to keep the analyses as simple as possible and isolate the effect of f_T, we keep the formulation of f_W constant in the experiments that follow.

2.2 Model setup and experiments

We configure the reduced complexity model in a spatially explicit way to represent global variations, implemented as a surrogate for the CASA-CNP biogeochemical module (Wang et al., 2010) of the CABLE land surface model (Wang et al., 2011). A previous simulation by CABLE coupled to the coarse-resolution CSIRO Mk3L climate model

(3.2° latitude ×5.6° longitude; Phipps et al., 2011) and driven by CMIP5 atmospheric CO_2 data provides monthly NPP, T_s and θ_s to the reduced complexity model. We use both historical simulations (Exbrayat et al., 2013b) and 21st century projections using the Representative Concentration Pathway 8.5 (RCP 8.5) atmospheric concentration scenario.

We perform a sensitivity analysis by running the simple model with various combinations of a Q_{10} value and a baseline residence time k. We use 11 equally-spaced values of Q_{10} ranging from 1.5 to 2.5 (i.e. intervals of 0.1), and 31 equally-spaced values of k ranging from 120 months to 480 months (i.e. intervals of 12 months). Each value of Q_{10} is applied with each value of k for a total of 341 simulations. Model versions are initialised via a classical spin-up procedure (Xia et al., 2012) using input data from 1850 to 1859 for 10 000 years to ensure all soil carbon pools reach a steady-state. We then continue simulations with NPP, T_s and θ_s data from 1850 to 2005, and continue with RCP 8.5 projections to 2100. In each model version, both k and the sensitivity of R_h to temperature (represented by Q_{10}) are constant globally, in accordance with observations (Mahecha et al., 2010) and state-of-the-art models (Todd-Brown et al., 2013; Nishina et al., 2013). However, the actual value of the environmental scalar f_T will of course vary spatially and temporally as a function of T_s. As we keep the same formulation of f_W between model versions, we can attribute differences in results to the values of Q_{10} or k.

2.3 Harmonized World Soil Database

The Harmonized World Soil Database (HWSD; FAO, 2012) combines several national inventories and provides a number of chemical and physical soil properties at a 30 arc second resolution globally. However, despite the availability of this dataset, CMIP5 models exhibit a six-fold range in their total soil carbon content (Todd-Brown et al., 2013) including values well outside the uncertainty boundaries of observational data. We showed previously that using this dataset to discriminate between acceptable and unacceptable simulations resulted in a non-negligible reduction of the uncertainty in historical net carbon uptake (Exbrayat et al., 2013b). While we do not aim to provide CMIP5-like projections of the soil carbon balance with our reduced complexity model, we investigate the value of using the HWSD to discriminate between plausible and implausible simulations.

We follow the method described by Todd-Brown et al. (2013) to derive an estimate of current total soil carbon from the latest version of the Harmonized World Soil Database (HWSD). First, we re-grid the original 30 arc seconds raster to a 0.5° × 0.5° resolution. Within each half-degree cell we select the dominant soil type. For each soil type, the database provides bulk density and organic carbon content for a top layer (0–30 cm depth) and a bottom layer (30–100 cm depth). This allows us to calculate soil C density (in $\mathrm{kg\,C\,m^{-2}}$) in each cell. We then multiply each grid cell by its area and sum to obtain a global estimate of ~ 1170 Pg C. Similarly to Todd-Brown et al. (2013) we also consider the uncertainty associated to our re-gridding process as well as analytical measurements of soil properties. We therefore obtain a 95 % confidence interval (CI_{95}) of 29 % below the mean to 32 % above the mean, or ~ 830–1550 Pg C. We provide these gridded data as Supplement.

3 Results

3.1 Total soil carbon and global balance

Figure 1 presents snapshots of total soil carbon for all 341 model versions for three periods: at equilibrium (in 1850, Fig. 1a), at the end of historical transient simulations (in 2005, Fig. 1b), and at the end of the projections with forcing corresponding to RCP 8.5 (in 2100, Fig. 1c). Figure 1a shows that the spin-up procedure causes different model versions to equilibrate at widely varying levels of total soil carbon despite the use of the same boundary conditions of NPP and T_s. Differences in residence time k contribute most of the ~ 592 to 2745 Pg C range, with larger values of k resulting in larger pools (Fig. 1a). Variations in the Q_{10} parameter of f_T have a smaller influence on total soil carbon but lower values do result in lower total soil carbon. For the same value of k, simulations with $Q_{10} = 1.5$ equilibrate with total soil carbon equal to $86\,\% \pm 0.005\,\%$ (mean ±1 standard deviation) of the amount with $Q_{10} = 2.5$. Figure 1b shows that the distribution of total soil carbon between model versions does not vary much during historical simulations (1850–2005). Models with large total soil carbon pools over this period remain versions with long residence time k and higher values of Q_{10}. Note, however, that the range of total soil carbon in 2005 grows to ~ 709 to 2943 Pg C. Dashed contours on Fig. 1b indicate the limits of the CI_{95} of the HWSD for current total soil carbon. Here, 115 simulations with values of k ranging approximately from 150 to 250 months all fall within this range for 2005, regardless of the Q_{10} value used. Finally, Fig. 1c continues to indicate a strong control of k on the total soil carbon in 2100. The projected range narrows to ~ 684 to 2825 Pg C throughout the 21st century. However, we note there is an inversion in the influence of Q_{10} on simulated total soil carbon with lower values of Q_{10} resulting in larger pools especially for longer baseline residence times k. Nevertheless, this is still minor compared to the influence of k on C_s.

Although the range in simulated soil carbon remains similar through time, non-negligible changes occur. This is highlighted in Fig. 2 which shows ΔC_s, the change in total soil carbon as a function of model parameters k and Q_{10} for the historical simulations (1850–2005, Fig. 2a) and RCP 8.5 projections (2006–2100, Fig. 2b). First, Fig. 2a clearly shows that all model versions act as a net carbon sink during historical simulations, accumulating between 81 and 283 Pg C. Model versions with longer residence time k tend to accumulate more carbon through time. However, models with the largest value of Q_{10} tend to accumulate only $69\,\% \pm 0.4\,\%$ (mean ±1 standard deviation) of the amount that the lowest Q_{10} models do. By analysing Fig. 2b, we see that the influence of Q_{10} on the total soil carbon balance grows during RCP 8.5 projections where Q_{10} now determines whether the soil remains a sink or becomes a source. This change between a source or a sink for different Q_{10} values follows a near linear relationship with k (solid line on Fig. 2b). Interestingly, the -179 to 168 Pg C range in the change in total soil carbon during RCP 8.5 is mostly a function of Q_{10} as both extremes are achieved with the longest residence time used here. In other words, while Q_{10} decides of the sign of the change, k drives the magnitude of the response.

If we consider only models that fall within the CI_{95} of the HWSD for current total soil carbon (dashed contours on Fig. 2a and b) the spread in simulated total soil carbon balance is significantly reduced. During the historical simulations, the range of this subset of models shrinks by 84 Pg C to between 87 and 205 Pg C. It corresponds to a reduction of about 42 % of the initial uncertainty. Similarly, the range in projected soil carbon balance is reduced by 157 Pg C to −129 to 61 Pg C, a reduction of about 45 % of the initial uncertainty. We note, however, that this restriction does not necessarily increase confidence in sign of the future soil carbon change under RCP8.5.

Differences in the behaviour between the full set of models and this subset of observationally constrained models can be seen in the time series and probability density functions (PDFs) for the historical period, shown in Fig. 3. First, the time series from 1850 shows there is no noticeable difference between the full set of simulations (in grey) and the subset of simulations with acceptable current soil carbon (in green) until 1900. During the first half of the 20th century, stronger sinks are excluded as they lie outside the CI_{95} range, which correspond to the upper tail of the distribution of ΔC_s (see PDF inset for 1950). However, the kurtosis of the distribution, or most probable change from our simulations, changes negligibly. After ~ 1960, we observe a step-change in cumulative ΔC_s that follows a strong response in NPP to the rapid increase in atmospheric $\mathrm{CO_2}$ (Exbrayat et al., 2013b). The spread between simulations grows and most of the excluded simulations based on the CI_{95} range are the strongest sinks (as in Fig. 2a) while a few of the least accumulating simulations are also excluded. This does have a large impact on the most probable change in storage, reducing it from ~ 200 PgC to ~ 140 PgC.

We now examine future simulations and present time series and PDFs of change in total soil carbon during RCP 8.5 projections in Fig. 4. All simulations continue to accumulate carbon at the beginning of the 21st century and remain net carbon sinks until about 2060. At the end of the century, some model versions have simulated positive

ΔC_s corresponding to a net carbon sink over the 21st century, while other ends their projections with negative ΔC_s, or a net carbon loss. However, all simulations show the same overall behaviour with first an increase in C_s that peaks, and then a decrease in C_s. The timing of the peak, i.e. when soil carbon starts to deplete, varies between ~ 2035 and 2080. This indicates that, in all simulations, soil has become a net source of carbon by the end of the 21st century, regardless how much carbon was accumulated since 2005, and hence since 1850. The PDFs in 2050 show that selecting only observationally consistent models results in the most heavily accumulating simulations, i.e. those that would peak later, to be dismissed. However, by 2100, both the lower and upper tails of the initial distribution are clipped, reducing the simulated range from -178 to 168 Pg C (all simulations) to -129 to 61 Pg C. In both cases, differences in the kurtosis of both distributions remains very small which indicates that our selection scheme dismisses outliers. We note that the lower bound of ΔC_s for both sets of models is the same until late in the projections (~ 2085).

3.2 Regional differences

Although Fig. 1 indicates that the range in k can explain most of the variability in total soil carbon content at equilibrium and hence through transient simulations, Q_{10} is likely to influence the local response of f_T. Figure 5 shows the relative value of f_T for different temperatures and values of Q_{10}. Since the chosen $T_{ref} = 15\,^{\circ}$C, all Q_{10} values lead f_T to be equal at this particular temperature. However, the more difference there is between the actual temperature and T_{ref}, the more sensitive f_T becomes to values of Q_{10}. As our simulations are spatially-explicit, this may introduce non-negligible regional differences in C pools at equilibrium and their response to transient changes in T_s and NPP.

To investigate this more in detail, we present the zonal averages of soil C density for different values of Q_{10} with k set to 180 months (Fig. 6). We choose this particular residence time as example because all corresponding simulations are within the CI_{95} of the HWSD for 2005 regardless the value of Q_{10}. Figure 6a shows that Q_{10} values do introduce non-negligible differences in local equilibrated soil C density. Steady-state pools at low latitudes (30° S to 30° N) are larger with low values of Q_{10} (blue in Fig. 6). Conversely, high latitude pools are larger with high values of Q_{10} (red in Fig. 6). Overall, the range in the value of zonally averaged soil C density at equilibrium is up to three-fold depending on the chosen value of Q_{10}. This is particularly obvious in regions with high NPP including low-latitude tropical rainforests or northern taigas. As was the case with total C_s, the zonal distribution soil C density and the relative position of simulations with different Q_{10} do not vary much between 1850 and 2005 (Fig. 6b) although there is a slight shift towards uniformly higher densities as all model versions are net global carbon sinks (Fig. 2a and 3). The pattern of zonal soil carbon remains essentially the same at the end of RCP 8.5 projections. However, models with lower values of Q_{10} now have more carbon than those with high values of Q_{10} over a broader zone (40° S–50° N).

Figure 7 shows the zonal change in soil C density for the same simulations as in Fig. 6. Figure 7a indicates that all simulations simulate a net sink almost everywhere during historical simulations, except at latitudes > 70° N. However, the strength of this sink is strongly dependent upon the value of Q_{10}, especially in low latitudes. There is an approximately two-fold difference between the high accumulation of low Q_{10} models, and the low accumulation of high Q_{10} models. Differences between Q_{10} values are negligible at higher latitudes. Figure 7b shows the same information for RCP 8.5 projections. Simulations with lower values of Q_{10} almost always accumulate more C (except between 0° and 10° N). While all model versions with $k = 180$ months lose carbon at low latitudes (20° S–20° N), and gain carbon at high latitudes in the Northern Hemisphere (> 50° N), the value of Q_{10}, and hence the environmental scalar f_T, decides of the sign of the local soil C balance in the 21st century at mid-latitudes. Within the mid-latitudes, high values of Q_{10} are more likely to simulate a net loss of soil carbon. We can therefore narrow down the dependence of the global ΔC_s on Q_{10} to its affect at mid-latitudes.

4 Discussion

4.1 Effect of k and Q_{10} on soil carbon

In our simulations, the range in total soil carbon at equilibrium (~ 592 to 2745 Pg C) depends on which value of Q_{10} and especially k is used (Fig. 1a). This range captures the ~ 561 to 2938 Pg C range in soil carbon in CMIP-5 in 1860 (see Fig. S1). We note of course that CMIP5 models not only vary in their soil C component, but simulate different NPP and T_s and also integrate a range of soil moisture limitations (Todd-Brown et al., 2013). The range achieved here at the end of the historical simulations (~ 709 to 2943 Pg C) is, for example, larger than the 1090 to 2646 Pg C range in 2000 from 7 DGVMs in the ISI-MIP project (Nishina et al., 2013) which were driven by a harmonised weather dataset.

We can attribute this range to the first-order representation of decomposition and its response to the initialisation procedure used in most CMIP-5 simulations. By spinning-up the model, the goal is to stabilise pools so that total NPP is exactly compensated by total R_h over the selected period of time (here 10 years). In Eq. (2), a longer residence time k results in a lower decay rate (i.e. R_h per unit of C_s). Therefore, model versions that have a slower turnover will require more substrate to simulate the same R_h needed to compensate NPP. As the baseline residence time k is applied globally, it drives the global pool size (Fig. 1) much more than changing Q_{10} affects f_T. However, as seen in Fig. 6, when considered regionally, Q_{10} plays a non-negligible role for the local response of decomposition and the definition of equilibrium soil C density. High values of Q_{10} lead f_T to trigger strong decay rates in warm regions (Fig. 5) that require less substrate (see low latitudes in Fig. 6a) to compensate the same NPP. Conversely, high Q_{10} lead to low values of f_T in cold regions. Therefore, more substrate is required to bring the pool to equilibrium as seen in high latitudes in Fig. 6a. Low values of Q_{10} show an opposite regional behaviour. Regional differences compensate each other and therefore f_T with different Q_{10} values can only explain a small fraction of the range in equilibrated total soil carbon. Of course, if another T_{ref} was used, the relative differences between f_T with different Q_{10} would be altered and the influence of Q_{10} and its effect on f_T on total and local C_s would vary.

Comparing Fig. 1a–c suggests that the range in total C_s at equilibrium is a good predictor of the current and future range in total soil carbon. Despite differences in the magnitude of the change in C_s through time (Friedlingstein et al., 2014), equilibrium conditions achieved under pre-industrial conditions largely define current and future pool sizes. Examining Fig. 6 confirms that this global effect can also be seen regionally, especially in low (20° S to 20° N) and high (> 50° N) latitudes, where carbon pools are largest. This is of concern as substrate availability also influences R_h and hence its response to changes.

Changes in C_s through time are nevertheless non-negligible, and it is important to quantify the response of the system to perturbations. Our results show increasing atmospheric CO_2 concentrations enhances NPP more than the simultaneous warming enhances R_h during historical simulations. This historical net carbon sink is in accordance with previous studies (Friedlingstein et al., 2006; Sarmiento et al., 2010; Zhang et al., 2011; Wania et al., 2012; Anav et al., 2013; Exbrayat et al., 2013b). Therefore, all model versions with longer residence time accumulate more C_s over the same time period as a result of a slower turnover of carbon in soils, and this mirrors the state of the equilibrium stores. However, despite the dominance of the increased NPP on ΔC_s, the historical warming signal is influential. Specifically, those model versions more sensitive to changes in temperature (i.e. with high values of Q_{10}) accumulate less soil carbon during the 20th century even though they initially equilibrated with larger global pools. This is also true of local soil C density where high Q_{10}values are less accumulating regardless of the initial soil C density.

Projections under the strong-forcing RCP 8.5 scenario also see an increase in the influence of the value of Q_{10} on ΔC_s. Figure 2b clearly shows that the capacity of soils to become carbon sources or remain sinks depends almost entirely on the Q_{10} parameter, and both states can be achieved for any value of k used while remaining within range of previous studies (Friedlingstein et al., 2014; Nishina et al., 2013). Figure 7b indicates that this is clearly a result of differences in the local response of model versions in the mid-latitudes as a function of Q_{10}. Such regional discrepancies leading to a change in the sign of global ΔC_s models have also been highlighted through a recent inter-comparison project that used a harmonised weather dataset to drive 7 biome models (Nishina et al., 2013). However, contrary to this previous study, none of our model versions accumulates soil carbon in the inter-tropical region during the 21st century. This is probably due to the fact that we use the same boundary conditions of NPP and T_s for all our model versions, while models used by Nishina et al. (2013) used a prescribed weather dataset but were left free to simulate their own NPP.

Overall, the globally applied model parameter$k$ drives the steady-state response of our reduced complexity system. However, the more conditions are changing (i.e. steady-state to historical to RCP 8.5 projections), the more the dynamic transition of the system towards a new equilibrium depends on the environmental scalar f_T and the specific value of Q_{10}. Although the same formulation of f_T is applied globally, differences in its response to local T_s sum up to determine the sign of total soil carbon balance. We also note that model versions that equilibrate as a result of longer baseline residence time k have a tendency to produce a larger absolute response of total soil carbon balance. This is counter logic, as higher values of k imply a smaller relative change in the decay rate $k^{-1} \times f_T \times f_W$ used in Eq. (2). Therefore, the size of pools to which the change is applied seems to dominate the response. This control of initial conditions obtained by spin-up on the response of the system is a critical aspect that needs to be better resolved, especially since recent inter-comparison experiments all exhibit huge discrepancies in equilibrium conditions of participating models (Anav et al., 2013; Todd-Brown et al., 2013; Nishina et al., 2013).

4.2 Discriminating between model versions

Since k clearly influences the total soil carbon content at equilibrium in 1850, it is a good predictor of the current total soil carbon content. Therefore, k is the key parameter that decides how much carbon is active in the modelled system, and whether model versions fall within the CI_{95} of the HWSD. Here, all simulations with baseline residence time between 150 and 250 months fulfil this requirement regardless of which Q_{10} is used in f_T.

If we isolate these simulations, the range in total soil carbon change shrinks by 42 % and 45 % for the historical simulations and RCP 8.5 projections, respectively. However, while this selection dismisses outliers it does not increase confidence in the sign of the soil carbon change. This is because regional differences lead to similar values in total soil carbon for different values of Q_{10}. These regional differences translate into heterogeneous responses under RCP 8.5 forcing, especially in mid-latitudes. They are sufficient to induce a change of sign in the global soil carbon balance.

5 Conclusion

We have used a reduced complexity model, broadly representative of the current state-of-the-art parameterization of soil organic C decomposition in CMIP-5 models, to explore the response of microbial decomposition to climate change on soil C dynamics at regional and global scale. We have shown that key parameters in the first-order representation of decomposition interact in markedly different ways depending on the nature of forcing and antecedent conditions. First, the time and space-invariant baseline residence time decides of the total soil carbon content at equilibrium after spin-up, typically the process used by CMIP5 models to initialise C pools. Next, the more boundary conditions imposed on the system move away from the equilibrium forcing, the more the environmental scalar describing the sensitivity of the system gains in importance. However, it is the size of the pool to which the change is applied that mostly controls the magnitude of the response.

Applying a constraint on total soil carbon that discriminates between acceptable simulations of total soil carbon leads to a drastic reduction of the range of simulated change. Meanwhile, most of the remaining uncertainty in 21st century projections of total soil carbon can be attributed to zonal differences in the response to change, especially at mid-latitudes. These do not allow us to confidently project soil as either a global source or sink of carbon for the 21st century. However, it is clear that under RCP 8.5 tropical soils are not suited for long-term carbon storage while some more potential exists in high latitudes.

Finally, we suggest that future estimates of terrestrial, and especially soil, carbon responses to climate change should be more constrained by available datasets of carbon stocks. This is crtictial as model parameterizations describe fluxes as a fraction of the substrate pool size. So far, the process of spin-up has too many degrees of freedom that lead to model-specific amounts of active soil carbon.

Supplementary material related to this article is available online at http://www.biogeosciences-discuss.net/11/4995/2014/ bgd-11-4995-2014-supplement.zip.

Acknowledgements. This work was supported by the Australian Research Council ARC grant DP110102618 and the ARC Centre of Excellence for Climate System Science grant CE110001028. CSIRO Mk3L model runs were made possible by the NCI National Facility at the Australian National University via the provision of computing resources to the ARC Centre of Excellence for Climate System Science.

References

Ahlström, A., Smith, B., Lindström, J., Rummukainen, M., and Uvo, C. B.: GCM characteristics explain the majority of uncertainty in projected 21st century terrestrial ecosystem carbon balance, Biogeosciences, 10, 1517–1528, doi:10.5194/bg-10-1517-2013, 2013.

Allison, S. D., Wallenstein, M. D., and Bradford, M. A.: Soil-carbon response to warming dependent on microbial physiology, Nat. Geosci., 3, 336–340, doi:10.1038/ngeo846, 2010.

Anav, A., Friedlingstein, P., Kidston, M., Bopp, L., Ciais, P., Cox, P., Jones, C., Jung, M., Myneni, R., and Zhu, Z.: Evaluating the land and ocean components of the global carbon cycle in the CMIP5 Earth systems models, J. Climate, 26, 6801–6843, doi:10.1175/JCLI-D-12-00417.1, 2013.

Bauer, J., Weihermüller, L., Huisman, J., Herbst, M., Graf, A., Séquaris, J., and Vereecken, H.: Inverse determination of heterotrophic soil respiration response to temperature and water content under field conditions, Biogeochemistry, 108, 119–134, doi:10.1007/s10533-011-9583-1, 2012.

Davidson, E. A. and Janssens, I. A.: Temperature sensitivity of soil carbon decomposition and feedbacks to climate change, Nature, 440, 165–173, doi:10.1038/nature04514, 2006.

Exbrayat, J.-F., Pitman, A. J., Abramowitz, G., and Wang, Y.-P.: Sensitivity of net ecosystem exchange and heterotrophic respiration to parameterization uncertainty, J. Geophys. Res.-Atmos., 118, 1640–1651, doi:10.1029/2012JD018122, 2013a.

Exbrayat, J.-F., Pitman, A. J., Zhang, Q., Abramowitz, G., and Wang, Y.-P.: Examining soil carbon uncertainty in a global model: response of microbial decomposition to temperature, moisture and nutrient limitation, Biogeosciences, 10, 7095–7108, doi:10.5194/bg-10-7095-2013, 2013b.

Falloon, P. D., Jones, C. D., Ades, M., and Paul, K.: Direct soil moisture controls of future global soil carbon changes: an important source of uncertainty, Global Biogeochem. Cy., 25, GB3010, doi:10.1029/2010GB003938, 2011.

FAO/IIASA/ISRIC/ISSCAS/JRC: Harmonized World Soil Database (version 1.21), FAO, Rome, Italy and IIASA, Laxenburg, Austria, 2012.

Friedlingstein, P., Cox, P., Betts, R., Bopp, L., von Bloh, W., Brovkin, V., Cadule, P., Doney, S., Eby, M., Fung, I., Bala, G., John, J., Jones, C., Joos, F., Kato, T., Kawamiya, M., Knorr, W., Lindsay, K., Matthews, H. D., Raddatz, T., Rayner, P., Reick, C., Roeckner, E., Schnitzler, K.-G., Schnur, R., Strassmann, K., Weaver, A. J., Yoshikawa, C., and Zeng, N.: Climate–carbon cycle feedback analysis: results from the C^4MIP Model Intercomparison, J. Climate, 19, 3337–3353, doi:10.1175/JCLI3800.1, 2006.

Friedlingstein, P., Meinhausen, M., Arora, V. K., Jones, C. D., Anav, A., Liddicoat, S. K., and Knutti, R.: Uncertainties in CMIP5 climate projections due to carbon cycle feedbacks, J. Climate, 27, 511–526, doi:10.1175/JCLI-D-12-00579.1, 2014.

Friend, A. D., Lucht, W., Rademacher T. T., Keribin, R., Betts, R., Cadule, P., Ciais, P., Clark, D. B., Dankers, R., Falloon, P. D., Ito A., Kahana, R., Kleidon, A., Lomas, M. R., Nishina, K., Ostberg, S., Pavlick, R., Peylin, P., Schaphoff, S., Vuichard, N., Warszawski, L., Wiltshire, A., and Woodward, F. I.: Carbon residence time dominates uncertainty in terrestrial vegetation responses to future climate and atmospheric CO_2, P. Natl. Acad. Sci. USA, 111, 3280–3285, doi:10.1073/pnas.1222477110, 2014.

Kirschbaum, M. U. F.: Soil respiration under prolonged soil warming: are rate reductions caused by acclimation or substrate loss?, Glob. Change Biol., 10, 1870–1877, doi:10.1111/j.1365-2486.2004.00852.x, 2004.

Knorr, W., Prentice, I. C., House, J. I., and Holland, E. A.: Long-term sensitivity of soil carbon turnover to warming, Nature, 433, 298–301, doi:10.1038/nature03226, 2005.

Koven, C. D., Ringeval, B., Friedlingstein, P., Ciais, P., Cadule, P., Khvorostyanov, D., Krinner, G., and Tarnocai, C.: Permafrost carbon-climate feedbacks accelerate global warming, P. Natl. Acad. Sci. USA, 108, 14769–14774, doi:10.1073/pnas.1103910108, 2011.

Lloyd, J. and Taylor, J. A.: On the temperature dependence of soil respiration, Funct. Ecol., 8, 315–323, doi:10.2307/2389824, 1994.

Luo, Y., Wan, S., Hui, D., and Wallace, L. L.: Acclimatization of soil respiration to warming in a tall grass prairie, Nature, 413, 622–625, doi:10.1038/35098065, 2001.

Mahecha, M. D., Reichstein, M., Carvalhais, N., Lasslop, G., Lange, H., Seneviratne, S. I., Vargas, R., Ammann, C., Arain, M. A., Cescatti, A., Janssens, I. A., Migliavacca, M., Montagnani, L., and Richardson, A. D.: Global convergence in the temperature sensitivity of respiration at ecosystem level, Science, 329, 838–840, doi:10.1126/science.1189587, 2010.

Nishina, K., Ito, A., Beerling, D. J., Cadule, P., Ciais, P., Clark, D. B., Falloon, P., Friend, A. D., Kahana, R., Kato, E., Keribin, R., Lucht, W., Lomas, M., Rademacher, T. T., Pavlick, R., Schaphoff, S., Vuichard, N., Warszawaski, L., and Yokohata, T.: Global soil organic carbon stock projection uncertainties relevant to sensitivity of global mean temperature and precipitation changes, Earth Syst. Dynam. Discuss., 4, 1035–1064, doi:10.5194/esdd-4-1035-2013, 2013.

Phipps, S. J., Rotstayn, L. D., Gordon, H. B., Roberts, J. L., Hirst, A. C., and Budd, W. F.: The CSIRO Mk3L climate system model version 1.0 – Part 1: Description and evaluation, Geosci. Model Dev., 4, 483–509, doi:10.5194/gmd-4-483-2011, 2011.

Sarmiento, J. L., Gloor, M., Gruber, N., Beaulieu, C., Jacobson, A. R., Mikaloff Fletcher, S. E., Pacala, S., and Rodgers, K.: Trends and regional distributions of land and ocean carbon sinks, Biogeosciences, 7, 2351–2367, doi:10.5194/bg-7-2351-2010, 2010.

Tarnocai, C., Canadell, J. G., Schuur, E. A. G., Kuhry, P., Mazhitova, G., and Zimov, S.: Soil organic carbon pools in the northern circumpolar permafrost region, Global Biogeochem. Cy., 23, GB2023, doi:10.1029/2008GB003327, 2009.

Taylor, K. E., Stouffer, R. J., and Meehl, G. A.: An overview of CMIP5 and the experiment design, B. Am. Meteorol. Soc., 93, 485–498, doi:10.1175/BAMS-D-11-00094.1, 2012.

Todd-Brown, K. E. O., Hopkins, F. M., Kivlin, S. N., Talbot, J. M., and Allison, S. D.: A framework for representing microbial decomposition in coupled climate models, Biogeochemistry, 109, 19–33, doi:10.1007/s10533-011-9635-6, 2012.

Todd-Brown, K. E. O., Randerson, J. T., Post, W. M., Hoffman, F. M., Tarnocai, C., Schuur, E. A. G., and Allison, S. D.: Causes of variation in soil carbon simulations from CMIP5 Earth system models and comparison with observations, Biogeosciences, 10, 1717–1736, doi:10.5194/bg-10-1717-2013, 2013.

Wang, Y. P., Law, R. M., and Pak, B.: A global model of carbon, nitrogen and phosphorus cycles for the terrestrial biosphere, Biogeosciences, 7, 2261–2282, doi:10.5194/bg-7-2261-2010, 2010.

Wang, Y. P., Kowalczyk, E., Leuning, R., Abramowitz, G., Raupach, M. R., Pak, B., van Gorsel, E., and Luhar, A.: Diagnosing errors in a land surface model (CABLE) in the time and frequency domains, J. Geophys. Res., 116, G01034, doi:10.1029/2010JG001385, 2011.

Wania, R., Meissner, K. J., Eby, M., Arora, V. K., Ross, I., and Weaver, A. J.: Carbon-nitrogen feedbacks in the UVic ESCM, Geosci. Model Dev., 5, 1137–1160, doi:10.5194/gmd-5-1137-2012, 2012.

Wieder, W. R., Bonan, G. B., and Allison, S. D.: Global soil carbon projections are improved by modelling microbial processes, Nat. Clim. Change, 3, 909–912, doi:10.1038/nclimate1951, 2013.

Xenakis, G. and Williams, M.: Comparing microbial and chemical approaches for modelling soil organic carbon decomposition using the DecoChem v1.0 and DecoBio v1.0 models, Geosci. Model Dev. Discuss., 7, 33–72, doi:10.5194/gmdd-7-33-2014, 2014.

Xia, J., Luo, Y., Wang, Y.-P., and Hararuk, O.: Traceable components of terrestrial carbon storage capacity in biogeochemical models, Glob. Change Biol., 19, 2104–2116, doi:10.1111/gcb.12172, 2013.

Xia, J. Y., Luo, Y. Q., Wang, Y.-P., Weng, E. S., and Hararuk, O.: A semi-analytical solution to accelerate spin-up of a coupled carbon and nitrogen land model to steady state, Geosci. Model Dev., 5, 1259–1271, doi:10.5194/gmd-5-1259-2012, 2012.

Zhang, Q., Wang, Y. P., Pitman, A. J., and Dai, Y. J.: Limitations of nitrogen and phosphorous on the terrestrial carbon uptake in the 20th century, Geophys. Res. Lett., 38, L22701, doi:10.1029/2011GL049244, 2011.

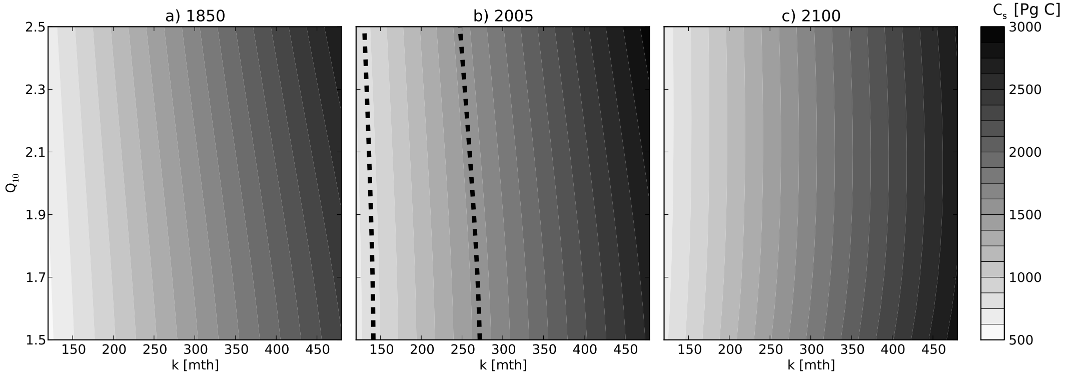

Fig. 1. Snapshots of total soil carbon in the reduced complexity model as a function of parameter values. Dashed contours in **(b)** indicate the CI_{95} of the HWSD in 2005 (830–1550 Pg C).

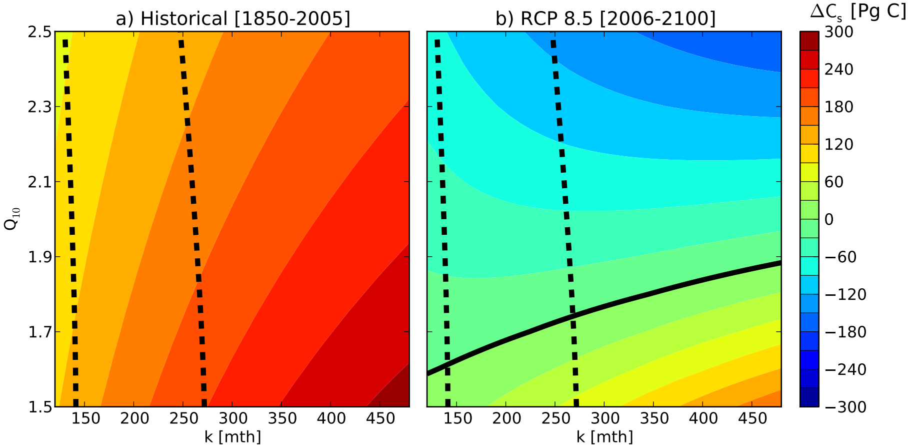

Fig. 2. Change in total soil carbon in the reduced complexity model as a function of parameter values for each period as indicated. Dashed contours in **(b)** indicate the CI_{95} of the HWSD in 2005 (830–1550 Pg C). The thick black line represents no change.

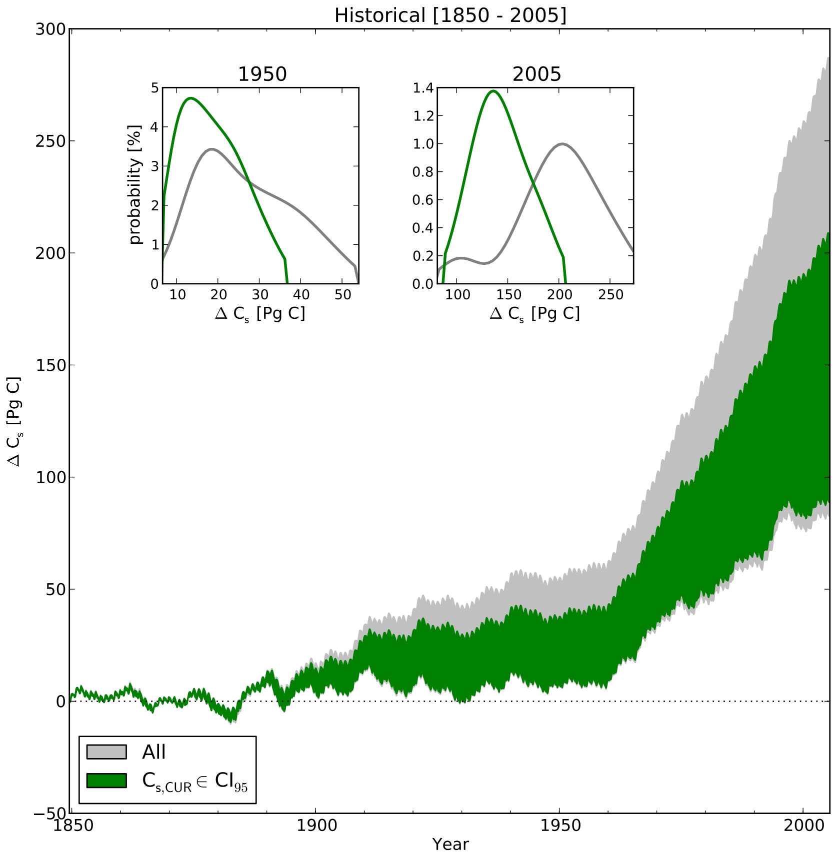

Fig. 3. Change in total soil carbon through time for historical simulations. Insets represent the probability density function of the change since 1850 for the period indicated. Grey is for all simulations while green is used to distinguish simulations for which total soil carbon is within the CI_{95} of the HWSD in 2005.

Title Page
Abstract | Introduction
Conclusions | References
Tables | Figures
◀| |▶
◀ ▶
Back | Close
Full Screen / Esc
Printer-friendly Version
Interactive Discussion

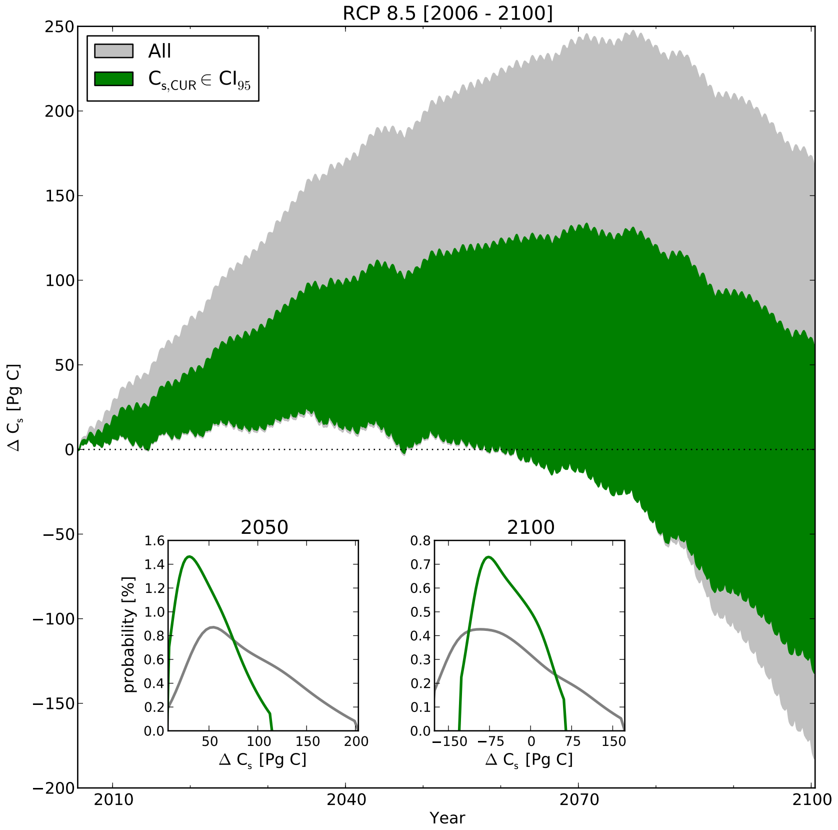

Fig. 4. Change in total soil carbon through time for RCP 8.5 projections. Insets represent the probability density function of the change since 2005 for the indicated year. Grey is for all simulations while green is used to distinguish simulations for which total soil carbon is within the CI_{95} of the HWSD in 2005.

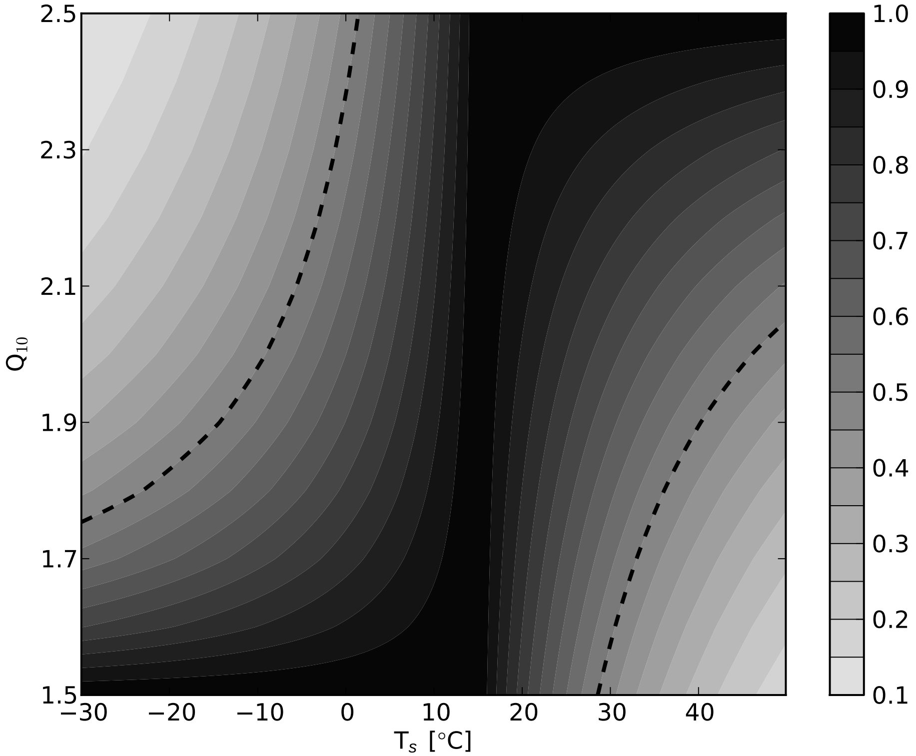

Fig. 5. Values of f_T as a function of T_s and Q_{10}. For each temperature, the value is expressed as the proportion of the maximum value achieved for any value of Q_{10}. Areas outside of the dashed lines represent where f_T is less than 50 % of the maximum for the same temperature.

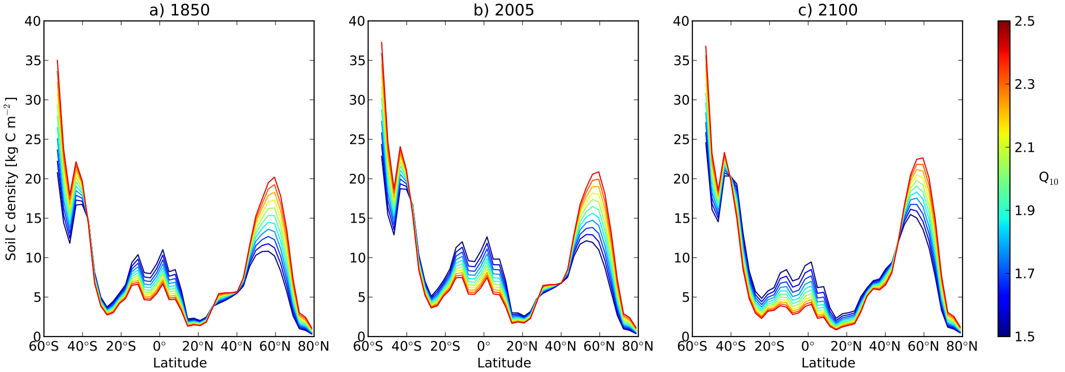

Fig. 6. Zonal average soil carbon density in the reduced complexity model with k = 180 months and various values of Q_{10} as indicated by the colour bar.

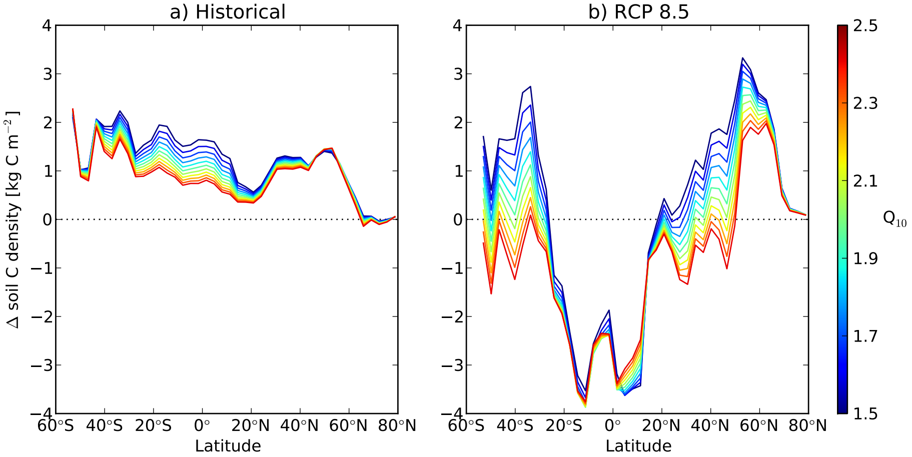

Fig. 7. Zonal change in soil C density during historical simulations **(a)** and RCP8.5 **(b)**.